Multiplicative Watermark Decoder in Contourlet Domain Using the Normal Inverse Gaussian Distribution

H. Sadreazami, *Student Member, IEEE,* M. Omair Ahmad, *Fellow, IEEE,* and M. N. S. Swamy, *Fellow, IEEE*

Abstract—In recent years, many works on digital image watermarking have been proposed all aiming at protection of the copyright of an image document or authentication of data. This paper proposes a novel watermark decoder in the contourlet domain. It is known that the contourlet coefficients of an image are highly non-Gaussian and a proper distribution to model the statistics of the contourlet coefficients is a heavy-tailed PDF. It has been shown in the literature that the normal inverse Gaussian (NIG) distribution can suitably fit the empirical distribution. In view of this, statistical methods for watermark extraction are proposed by exploiting the NIG as a prior for the contourlet coefficients of images. The proposed watermark extraction approach is developed using the maximum likelihood method based on the NIG distribution. Closed-form expressions are obtained for extracting the watermark bits in both clean and noisy environments. Experiments are performed to verify the robustness of the proposed decoder. The results show that the proposed decoder is superior to other decoders in terms of providing a lower bit error rate. It is also shown that the proposed decoder is highly robust against various kinds of attacks such as noise, rotation, cropping, filtering and compression.

Index Terms—Digital image watermarking, contourlet transform, normal inverse Gaussian distribution, watermark extraction.

I. INTRODUCTION

DIGITAL image watermarking has become a necessity in many applications such as data authentication, broadcast monitoring on the Internet and ownership identification [1]-[4]. Various watermarking schemes have been proposed to protect the copyright information [4]-[10]. There are three indispensable, yet contrasting requirements for a watermarking scheme: robustness, invisibility and capacity. Therefore, a watermarking scheme should provide a trade-off between these features. The watermarking techniques can be categorized in different ways based on (1) the embedding domain: pixel [5], [6] or frequency [7]-[16], (2) the embedding method: additive [8], [12], [14], [17], multiplicative [7], [10], [11], [15] or based on quantization [18], and (3) the extraction or detection methods: blind [7], [8], or non-blind [16], [17]. It has been shown that the multiplicative watermarking schemes are more

robust and provide higher imperceptibility of the watermark than the additive ones [11]. Therefore, detection and extraction of the multiplicative watermarks have received a great deal of attention [7], [11], [16].

A watermarking scheme should be robust against any intentional or unintentional distortion, and only an authorized user should be able to detect the watermark. The robustness can be significantly increased by utilizing the spread spectrum technique [3], [7], [17] in which the watermark is embedded in transform domains such as the discrete cosine transform [9], [14], discrete wavelet transform [8], [13], [15], [20], finite ridgelet transform [17], curvelet transform [21], or the contourlet transform [7], [16], [22]-[27]. Recently, a number of watermarking schemes have been proposed, wherein the watermark is embedded into the contourlet coefficients of an image. It has been shown that the contourlet-domain watermarking techniques are more robust than other frequency-domain watermarking algorithms against attacks [7], [24], [27].

Extraction of the watermarks can be achieved by using statistical methods. Therefore, choosing an appropriate statistical model is of great importance. It is known that to design a statistical watermark decoder, the correlation-based method is not optimal for non-Gaussian transform domain coefficients and thus, other alternative optimum and locally optimum detectors and decoders have been proposed [7]-[12], [14]-[16], [28]. In these works, the coefficients are assumed to be independent and identically distributed as the generalized Gaussian (GG) [16], [29], Laplacian [15], Gausse-Hermite [8], Cauchy [7], [21], K-Bessel function [28], Beta distribution [30], alpha-stable distributions [7], [14], [31], Gaussian mixture model [32] and normal inverse Gaussian distributions [33]-[35].

In [28], a locally-optimum watermark detector for additive watermarks using the Bessel K form distribution has been proposed. In [30], an optimum watermark decoder has been proposed by modeling the noisy watermarked dihedral angles by the Beta distribution. A watermark decoder has been designed in [36] by modeling the wavelet coefficients of images using the Gaussian distribution.

It is known that the contourlet coefficients of images have significant non-Gaussian statistics, i.e., having large peaks around zero and tails heavier than that of a Gaussian probability density function (PDF) [7], [30]. In view of this, these coefficients have been so far modeled by the non-Gaussian distributions such as the GG, alpha-stable and Cauchy PDFs. Accordingly, statistical watermark detectors by using the

alpha-stable [7] and GG [16] PDFs, and watermark decoder using the GG PDF [16] have been proposed.

It is shown in [33] that the normal inverse Gaussian (NIG) PDF can also be used to model the contourlet coefficients of images, since this distribution provides a very close fit to the distribution of the contourlet coefficients of images. In watermarking application, this distribution has been used to design a watermark detector for additive watermarks in the wavelet domain [34]. However, there exist no work on multiplicative watermark decoder in the contourlet domain using the NIG distribution. In view of this and in order to achieve higher robustness against various kinds of attacks, in this work, a new statistical multiplicative watermark decoder is designed based on the NIG distribution. The optimum watermark decoder in the contourlet domain is designed by using the maximum likelihood method. Closed-form expressions of the proposed decoder are obtained for extracting the watermark bits in both clean and noisy environments. Experiments are performed to assess the performance of the proposed NIG-based decoder and to compare it with those obtained using other existing works. The robustness of the proposed watermarking scheme is examined when the watermarked images are attacked by JPEG compression, Gaussian noise, salt & pepper noise, median filtering, Gamma correction, rotation, cropping and scaling.

The paper is organized as follows: Sections II presents a brief review of the contourlet transform and the normal inverse Gaussian distribution. In Section III, watermark embedding procedure is discussed and a watermark decoder based on the NIG model is designed. In Section IV, the performance of the proposed watermarking decoder is examined. Section V concludes the paper.

II. CONTOURLET TRANSFORM

The contourlet transform, a new image decomposition scheme proposed in [37], provides an efficient representation for two-dimensional signals with smooth contours and in this case outperforms the wavelet transform, which fails to recognize the smoothness of the contour. In addition, contourlet transform offers a higher degree of directionality with better sparseness. There are number of other structures such as the complex wavelet [38], ridgelet [17], [39] and curvelet [21], [40] that also provide multiscale and directional image representation. However, these structures are not flexible in the sense that they do not permit for different number of directions at each scale. Moreover, since the contourlet transform has been introduced in the discrete domain, it overcomes the blocking artifact drawback of the curvelet transform and is computationally more efficient. In the contourlet transform, the Laplacian pyramid filter captures the point singularities, which are contained in the residual signal. This residual signal is then passed through a directional filter bank that decomposes it into several directions to obtain directional information. This process is repeated by decomposing the coarse version to obtain directional subbands at multiple scales. The schematic structure of the analysis part of the contourlet transform is shown in Fig. 1.
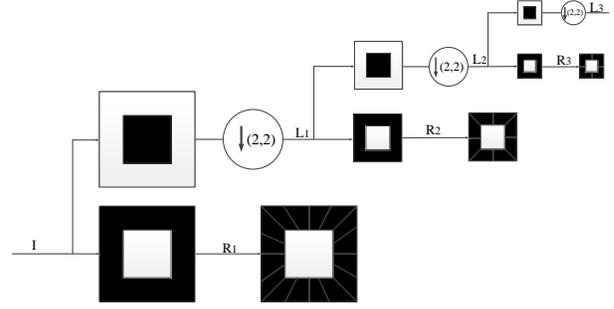
Fig. 1. Block diagram of the contourlet filter bank structure. The Laplacian pyramid is applied to the original image in order to have multiscale decomposition where the coarse image, denoted by L, is iteratively subsampled and each residual image, denoted by R, is fed into directional filter bank to obtain directional information. The scheme is flexible since it allows for a different number of directions at each scale.

There are many works on image watermarking showing that the performance of the contourlet-domain algorithms is superior to that of the wavelets [7], [24], [27]. This is mostly due to the fact that the contourlet transform captures more directional information and has better sparseness properties. These make the contourlet-domain watermarking algorithms more resistant to attacks. In recent years, statistical properties of the contourlet coefficients have received great attention and used in many image processing applications such as image watermarking [7], [16]. In has been shown that the contourlet coefficients of an image are highly non-Gaussian [29], [32], [41], i.e., having large peaks around zero and tails heavier than that of a Gaussian PDF. Therefore, a proper distribution to model the statistics of the contourlet coefficients would be a heavy-tailed PDF. It is shown in [33] that the NIG PDF provides a very close fit to the contourlet coefficients of images. The NIG distribution can be presented by a mixture of two independent distributions as [42],

$$X = \mu + \beta Z + \sqrt{Z} Y \qquad (1)$$

where $Y \sim N(0,1)$ is the Gaussian and $Z \sim IG(\delta, \gamma)$ is the inverse Gaussian distributions, respectively. It follows from (1) that $X|Z = z \sim N(\mu + \beta z, z)$ [42]. The IG PDF is then given by [43]

$$f_{IG}(z) = \frac{\delta e^{\delta \gamma} z^{-3/2}}{\sqrt{2\pi}} \exp\left\{ \frac{-1}{2} \left(\frac{\delta^2}{z} + \gamma^2 z \right) \right\} \qquad (2)$$

The NIG density function is then given by [44], [45],

$$f_{NIG}(x) = \frac{\alpha \delta e^{\delta \gamma + \beta(x-\mu)}}{\pi} \frac{K_1\left(\alpha \sqrt{\delta^2 + (x-\mu)^2} \right)}{\sqrt{\delta^2 + (x-\mu)^2}} \qquad (3)$$

where $K_\lambda(x)$ is a modified Bessel function of the second kind with index λ and $\gamma = \sqrt{\alpha^2 - \beta^2}$. The shape of the NIG distribution is specified by the parameter α, while β, μ and δ are skewness, location, and scale parameters, respectively. The parameters are bound as $0 \leq |\beta| < \alpha$, $\delta > 0$ and $-\infty < \mu < \infty$. The steepness of the PDF is controlled by α in that, as it is increased, the PDF becomes steeper. For a zero-mean and symmetric data distribution, $\mu = \beta = 0$.
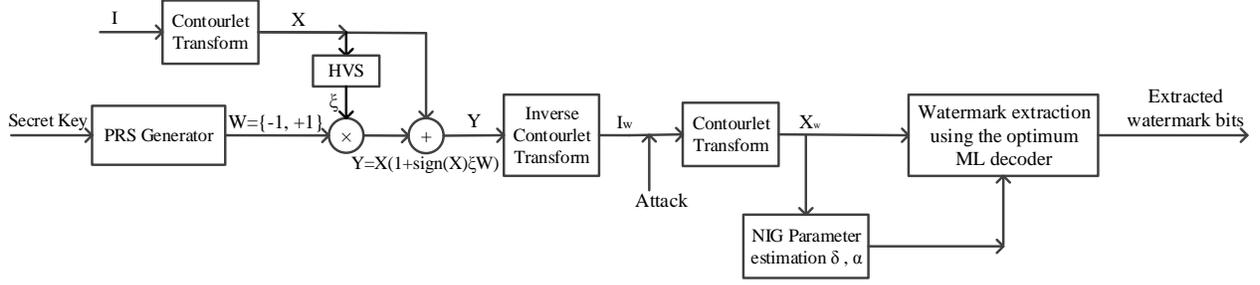
Fig. 2. Block diagram of the watermarking procedure. I and I_w denote the original and watermarked images, respectively.

III. WATERMARKING

A. Watermark embedding

In view of the fact that the multiplicative watermarks are image content dependent [11], and thus more robust than additive watermarks, in our proposed watermarking scheme, we embed the watermark bits in a multiplicative spread spectrum approach in the contourlet domain. The contourlet transform is first applied to an image to capture the important features of the image in a few coefficients. In case of a single bit watermarking scheme, let $\mathbf{x} = \{x_1, ..., x_N\}$ be the magnitude of a set of contourlet coefficients of the host image and $\mathbf{w} = \{w_1, ..., w_N\}$ be a pseudo-random sequence taking values $\{-1, 1\}$. The set of watermarked coefficients $\mathbf{y} = \{y_1, ..., y_N\}$ is obtained by

$$y_i = (1 + sign(x_i)\xi w_i)\, x_i, \ i = 1, ..., N \qquad (4)$$

where ξ is a positive weighting factor used to provide a trade-off between the robustness of the watermarking scheme and the imperceptibility of the embedded watermark based on the local characteristics of the image. The watermark is generated using a pseudo-random sequence generator with an authentication key as its initial value. This pseudorandom sequence spreads the spectrum of the watermark signal over many coefficients making it difficult to be detected for unauthorized users. To maximize the security and robustness of the watermarking scheme, the sequence should have whitenoise like properties [8]. A basic assumption is that the statistical distribution of the contourlet coefficients is not altered after embedding the watermark. This assumption is naturally justified by the fact that the embedded watermark is imperceptible. When the watermark carries a message, i.e., multibit watermarking scheme, binary bits of 0 or 1 are embedded as

$$y_{i|1} = (1 + sign(x_i)\xi)\, x_i, \ 1 \ is \ embedded$$
$$y_{i|0} = (1 - sign(x_i)\xi)\, x_i, \ 0 \ is \ embedded \qquad (5)$$

It should be mentioned that ξ can be increased to a point where the watermark is still invisible, and yet it is still detectable. The watermarked contourlet coefficients are then inverse transformed to get the watermarked image. Fig. 2 depicts the block diagram of the proposed watermark embedding and decoding procedures.

B. Watermark decoder

In a multi-bit watermarking scheme, the role of a decoder is to extract the hidden binary sequence from a set of observed contourlet coefficients. In our watermarking scheme, the bits of the binary sequence are assumed to be equally probable and the contourlet coefficients are assumed to be independent and identically distributed by the NIG distribution. In this work, to extract the hidden bits in the contourlet subband coefficients, we develop an optimum decoder based on the NIG PDF. To this end, for a subband with N coefficients, the maximum likelihood decision can be formulated as

$$f_{NIG}(y_1, y_2, ..., y_N|1) \mathop{\gtrless}_{0}^{1} f_{NIG}(y_1, y_2, ..., y_N|0) \qquad (6)$$

in which

$$f_{NIG}(\mathbf{y}|1) = \frac{\alpha\delta e^{\alpha\delta}}{\pi} \frac{K_1\left(\alpha\sqrt{\delta^2 + \left(\frac{\mathbf{y}}{1+sign(\mathbf{y})\xi}\right)^2}\right)}{\sqrt{\delta^2 + \left(\frac{\mathbf{y}}{1+sign(\mathbf{y})\xi}\right)^2}} \qquad (7)$$

and

$$f_{NIG}(\mathbf{y}|0) = \frac{\alpha\delta e^{\alpha\delta}}{\pi} \frac{K_1\left(\alpha\sqrt{\delta^2 + \left(\frac{\mathbf{y}}{1-sign(\mathbf{y})\xi}\right)^2}\right)}{\sqrt{\delta^2 + \left(\frac{\mathbf{y}}{1-sign(\mathbf{y})\xi}\right)^2}} \qquad (8)$$

The decision is simplified as

$$\sum_{i=1}^{N} ln \frac{\sqrt{\delta^2 + (\frac{y_i}{1-sign(y_i)\xi})^2}\, K_1\left(\alpha\sqrt{\delta^2 + (\frac{y_i}{1+sign(y_i)\xi})^2}\right)}{\sqrt{\delta^2 + (\frac{y_i}{1+sign(y_i)\xi})^2}\, K_1\left(\alpha\sqrt{\delta^2 + (\frac{y_i}{1-sign(y_i)\xi})^2}\right)} \mathop{\gtrless}_{0}^{1} T$$

$$(9)$$

where $T = \sum_{i=1}^{N} ln \frac{1+sign(y_i)\xi}{1-sign(y_i)\xi}$.

C. Watermark decoder in presence of noise

The watermarked coefficients y_i may be contaminated by zero mean additive white Gaussian noise $n \sim N(0, \sigma_n^2)$ as

$$z_i = \underbrace{(1 + sign(x_i)\xi w_i)\, x_i}_{y_i} + n \qquad (10)$$

3

Considering the independence assumption of the noise and the observation, the density function of the noisy contourlet coefficients can be obtained as

$$f_z(\mathbf{z}) = \int_{-\infty}^{\infty} f_y(\mathbf{z} - \tau) f_n(\tau) d\tau \qquad (11)$$

where

$$f_y(y) = \frac{1}{1 + sign(y)\xi w} f_x \left(\frac{y}{1 + sign(y)\xi w} \right) \qquad (12)$$

To simplify (11), we can estimate the Gaussian PDF using the three-sigma rule [16], [46]-[48]

$$f_n(n) = \begin{cases} \frac{-n+3\sigma_n}{9\sigma_n^2} & 0 < n \le 3\sigma_n \\ 0 & |n| > 3\sigma_n \\ \frac{n-3\sigma_n}{9\sigma_n^2} & -3\sigma_n \le n < 0 \end{cases} \qquad (13)$$

By substituting (13) in (11) and using the Simpsons integration approximation rule (See appendix A), we have

$$f(\mathbf{z}) = \frac{\sigma_n}{4} [2f_{NIG}(\mathbf{z})f_n(0) + 4f_{NIG}(\mathbf{z} - \frac{3\sigma_n}{2})f_n(\frac{3\sigma_n}{2})$$
$$+ 4f_{NIG}(\mathbf{z} + \frac{3\sigma_n}{2})f_n(\frac{-3\sigma_n}{2}) + f_{NIG}(\mathbf{z} + 3\sigma_n)f_n(-3\sigma_n)$$
$$+ f_{NIG}(\mathbf{z} - 3\sigma_n)f_n(3\sigma_n)] \qquad (14)$$

which can be simplified to

$$f(\mathbf{z}) = \frac{1}{6} \left(f_{NIG}(\mathbf{z} - \frac{3\sigma_n}{2}) + f_{NIG}(\mathbf{z}) + f_{NIG}(\mathbf{z} + \frac{3\sigma_n}{2}) \right) \qquad (15)$$

Therefore, for $f_{NIG}(\mathbf{z}|1)$ and $f_{NIG}(\mathbf{z}|0)$ we respectively have

$$f(z_1, z_2, ..., z_N|1) = \prod_{i=1}^{N} f(z_i|1)$$
$$= \frac{1}{6} \prod_{i=1}^{N} [f_{NIG,1}(z_i - \frac{3\sigma_n}{2}) + f_{NIG,1}(z_i) + f_{NIG,1}(z_i + \frac{3\sigma_n}{2})] \qquad (16)$$

and

$$f(z_1, z_2, ..., z_N|0) = \prod_{i=1}^{N} f(z_i|0)$$
$$= \frac{1}{6} \prod_{i=1}^{N} [f_{NIG,0}(z_i - \frac{3\sigma_n}{2}) + f_{NIG,0}(z_i) + f_{NIG,0}(z_i + \frac{3\sigma_n}{2})] \qquad (17)$$

where $f_{NIG,1}$ and $f_{NIG,0}$ are computed from (7) and (8), respectively. It is seen from (15) that the ML decision depends on the noise standard deviation σ_n. To obtain an estimation of the noise, we use the median estimator on the observed contourlet coefficients of different scales and directions as [49]

$$\hat{\sigma}_{n(j,d)} = \frac{Median|y_{j,d}|}{0.6745} \qquad (18)$$

where $y_{j,d}$ denotes the contourlet subband coefficients in the jth, $j = 1, ..., J$ scale and dth, $d = 1, ..., D$ direction.

	PSNR (dB)		BER (%)	
	9-7	pkva	9-7	pkva
Barbara	52.38	52.10	7.9	11.5
Lena	55.58	55.13	6.1	9.8
Baboon	51.47	50.94	7.8	10.4
Boat	54.38	53.73	5.9	8.4

IV. EXPERIMENTAL RESULTS

Experiments are performed to evaluate the imperceptibility of the embedded watermark as well as the robustness of the proposed watermarking scheme against various attacks. In our experiments, we use two set of grayscale images of size 512×512, obtained from [50] and [51]. The original images are first decomposed into a number of subbands by using the contourlet transform with two pyramidal levels followed by eight directions in each scale. We then select the subband with the highest variance in the finest scale to embed the watermark bits in a multiplicative manner, as in (4). The results are obtained by averaging over 100 runs with 100 different pseudorandom sequences as the watermark bits. For both stages of the contourlet transform, two different contourlet filters are considered, namely, the ladder filters, i.e., *pkva* and $9 - 7$ bi-orthogonal filters.

Table I gives the peak signal-to-noise-ratio (PSNR) and bit error rate (BER) values obtained using the proposed watermarking scheme with two different contourlet filters for some of the test images. It is seen from this Table that the $9 - 7$ biorthogonal filter is a better choice in our watermarking scheme, since it provides higher PSNR values for the watermarked images along with lower BER when the watermarked images are contaminated by Gaussian noise with $\sigma_n = 30$. Therefore, we obtain the rest of the results using $9 - 7$ biorthogonal filters. The original and watermarked images for two of the test images, namely, *Barbara* and *Lena*, as well as the absolute difference between the watermarked and the original image are shown in Fig. 3. The PSNR values between the original and watermarked *Barbara* and *Lena* images are 52.38 and 55.58 dB, respectively. The images are indistinguishable, thus showing the effectiveness of the contourlet-domain multiplicative watermarking scheme in terms of the invisibility of the watermark.

It should be noted that the PDFs of the original and watermarked images are assumed to be the same, i.e., embedding the watermark with small ξ does not change the distribution of the original image coefficients [9], [14]. Therefore, the parameters of NIG distribution can be estimated from observation $\mathbf{y}$. For the proposed NIG-based watermarking scheme, the only required side information is 8 bits data for the watermark strength ξ. In order to validate the theoretical expressions of the proposed decoder in noisy environment, we compare the experimental and theoretical BER values for a watermark strength ξ varying from 0.001 to 1. Fig. 4 shows the theoretical and experimental BER values averaged over 3000 images obtained using the proposed decoder in noisy environment with

Fig. 3. (a) Original, (b) watermarked test images of *Barbara*, PSNR=52.38 dB, and *Lena*, PSNR=55.58 dB, and (c) the difference between the original and watermarked images obtained using the proposed watermarking scheme.
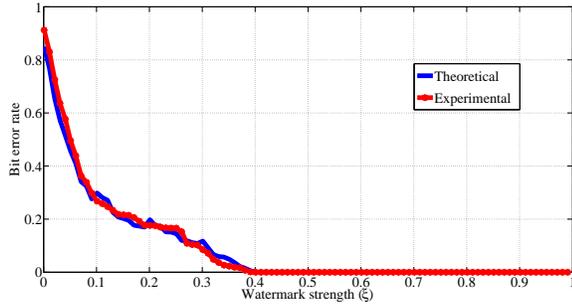
Fig. 4. Theoretical and experimental BER of the extracted watermark obtained using the proposed decoder for watermark strengths varying from 0.001 to 1, averaged over 3000 images obtained from [51].

Fig. 5. BER values of the extracted watermark obtained using the proposed NIG-based decoder and the GG-based decoder in [16] under the JPEG compression attack with different quality factors.

$\sigma_n = 40$. It is seen from this figure that the experimental BER is very close to the theoretical one indicating the validity of the theoretical results obtained using (15). It is also seen from this figure that the proposed decoder is very resistant to Gaussian noise especially for $\xi > 0.3$. We now examine the performance of the proposed watermark decoder in the contourlet domain by using the NIG distribution and compare it to those yielded by using the Cauchy and GG-based decoders with and without attacks. Table II gives BER values obtained using the proposed NIG-based decoder as well as that obtained using the Cauchy and GG-based decoders with message lengths of 128 or 256 bits for three of the test images, namely, *Barbara*, *Lena* and *Boat*, with and without attack. The attacks considered in this experiment are JPEG compression with $QF = 30$ and 40, AWGN with standard deviation $\sigma_n = 10$ and 20, median and Gaussian filtering with windows sizes 3×3 and 7×7, Gamma correction with $\gamma = 0.5$ and 2, rotation with $\theta = -5°$ and $5°$,

salt & pepper noise with $p = 5\%$ and 10%, and 5% and 15% cropping. It is seen from this table that the proposed NIG-based decoder provides a lower BER value than the other decoders do, in the presence or absence of any attack. Similar results are also obtained for other test images.

We now compare the performance of the proposed NIG-based decoder in the contourlet domain with that yielded by other existing works such as [16], [19], [20], [30], [36] and [52]-[55]. In order to make a fair comparison, we consider the same message length and PSNR values in our experiments as the message length and PSNR values used in other works. Fig. 5 shows BER values of the extracted watermark obtained using the proposed decoder and that obtained using the decoder in [16] for the test images, *Barbara*, *Baboon*, *Couple* and *Bridge*, when the watermarked image is JPEG-compressed with QFs from 30 to 90. It is seen from this figure that the proposed decoder is more robust than that in [16] in terms of providing

TABLE II

BIT ERROR RATES (%) OBTAINED USING THE PROPOSED NIG-BASED DECODER AS WELL AS THE CAUCHY AND GG-BASED DECODERS UNDER DIFFERENT ATTACKS. (BEST RESULTS ARE SHOWN IN BOLD)

	Barbara			Lena			Boat		
	NIG	Cauchy	GG	NIG	Cauchy	GG	NIG	Cauchy	GG
Message length=128 bits									
No attack	**0**	0	0.6	**0**	0.3	1.2	**0**	0	0.5
JPEG $QF = 30$	**23.2**	24.4	26.1	**21.3**	22.2	25.3	**20.1**	21.1	24.4
JPEG $QF = 40$	**18.5**	23.2	24.2	**17.7**	18.7	19.8	15.2	**15.0**	19.3
AWGN $\sigma_n = 10$	1.7	**1.3**	3.1	**1.5**	1.9	2.9	1.9	**1.8**	2.9
AWGN $\sigma_n = 20$	4.9	**4.6**	7.7	**3.8**	4.1	6.4	3.3	**3.2**	6.8
Median filter 3×3	**2.4**	3.2	5.2	**2.2**	3.4	5.0	**2.5**	2.7	4.8
Median filter 7×7	**8.2**	9.5	9.8	**7.9**	9.7	10.8	**7.5**	8.1	8.9
Gaussian filter 3×3	**0**	0	1.3	**0**	1.2	1.7	**0**	0	1.3
Gaussian filter 7×7	**1.1**	1.5	3.0	**1.3**	2.0	3.3	**1.3**	1.5	3.1
Gamma correction $\gamma = 2$	**0**	0	0.3	**0**	0.1	0.3	**0**	0	0.2
Gamma correction $\gamma = 0.5$	**3.4**	4.5	4.6	**3.1**	4.1	4.6	**2.7**	3.7	4.3
Cropping 5%	**0.9**	1.1	1.5	**0.5**	0.8	1.2	1.2	**1.1**	1.9
Cropping 15%	**6.2**	6.8	9.5	**6.1**	6.5	8.2	8.4	**8.1**	9.7
Rotation $-5°$	2.7	**2.6**	3.1	**2.9**	3.1	3.7	**1.6**	1.8	2.5
Rotation $5°$	**2.1**	2.2	3.0	**2.4**	2.5	3.1	**1.9**	2.2	2.9
Salt & pepper 5%	**2.9**	3.1	3.6	**2.8**	2.8	3.4	**5.2**	5.4	5.9
Salt & pepper 10%	**4.2**	4.5	5.1	**4.5**	4.6	5.7	**7.9**	8.2	9.2
Message length=256 bits									
No attack	**0**	0	0.9	**0**	0.6	1.6	**0**	0	0.7
JPEG $QF = 30$	**28.1**	30.5	32.3	**24.2**	28.5	29.9	**23.1**	23.7	28.9
JPEG $QF = 40$	**24.8**	27.3	29.1	**22.4**	25.6	27.8	**20.8**	21.6	24.8
AWGN $\sigma_n = 10$	**2.3**	2.4	3.4	**2.0**	2.4	4.2	2.8	**2.6**	4.5
AWGN $\sigma_n = 20$	**5.4**	5.8	9.9	**6.3**	6.5	10.8	6.1	**6.0**	9.4
Median filter 3×3	**4.3**	5.4	7.1	**4.2**	5.8	7.7	**4.3**	4.8	8.9
Median filter 7×7	**12.8**	14.2	15.5	**11.7**	13.6	14.3	12.5	**12.4**	15.9
Gaussian filter 3×3	**0**	0	2.3	**0**	2.1	2.6	**0**	0	1.9
Gaussian filter 7×7	**1.5**	2.3	4.5	**1.7**	3.8	4.6	**1.6**	1.9	3.7
Gamma correction $\gamma = 2$	**0**	0.3	0.6	**0**	0.2	0.7	**0**	0	0.3
Gamma correction $\gamma = 0.5$	**4.1**	5.7	6.9	**4.3**	5.8	7.2	**3.9**	5.1	6.7
Cropping 5%	3.4	**3.2**	4.1	**3.1**	3.2	4.2	4.1	**4.0**	5.1
Cropping 15%	9.3	**9.1**	11.5	**8.9**	9.1	11.2	**9.8**	9.8	12.4
Rotation $-5°$	**3.9**	4.2	5.4	**4.3**	4.8	5.6	**3.1**	3.2	5.0
Rotation $5°$	**2.1**	2.2	3.0	**2.4**	2.5	3.1	**1.9**	2.2	2.9
Salt & pepper 5%	**4.5**	4.9	5.9	**4.5**	4.6	5.8	**8.1**	8.5	9.1
Salt & pepper 10%	**7.4**	7.6	8.2	**7.5**	7.7	8.3	**12.2**	12.7	14.3
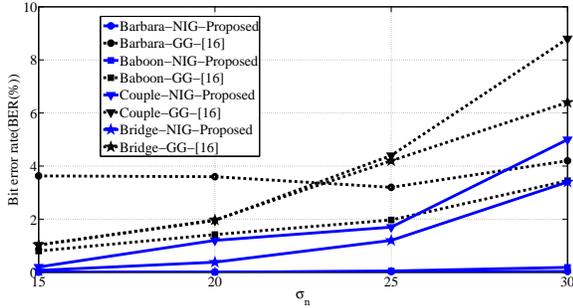
Fig. 6. BER of the extracted watermark using the proposed NIG decoder and the GG-based decoder in [16] under the AWGN attack with different noise levels.

TABLE III
BIT ERROR RATES (%) OBTAINED USING THE PROPOSED SCHEME AND THAT OBTAINED USING THE SCHEMES IN [36], [52] AND [53], UNDER AWGN WITH VARIOUS NOISE LEVELS FOR *Lena* IMAGE (PSNR = 45 *dB*).

	σ_n					
	5	10	15	20	25	30
Balado [52]	0	8.91	16.46	38.91	54.93	64.12
VLQIM [53]	0.27	8.50	14.27	29.20	40.58	52.08
GM [36]	3.34	8.23	13.84	18.45	23.58	27.52
Proposed	0	0	1.15	2.45	3.72	6.1

TABLE IV
BIT ERROR RATES (%) OBTAINED USING THE PROPOSED WATERMARKING SCHEME AS WELL AS THAT OBTAINED USING THE SCHEMES IN [19] AND [30], UNDER AWGN WITH $\sigma_n = 10$ AND 30, FOR *Lena*, *Baboon* AND *Peppers* IMAGES (MESSAGE LENGTH = 256 BITS).

	σ_n					
	10			30		
	Proposed	[30]	[19]	Proposed	[30]	[19]
Lena	0.6	5.01	1.85	5.7	20.11	26.39
Baboon	0.9	6.13	1.28	6.1	23.11	26.28
Peppers	1.1	3.62	1.32	7.0	18.81	25.92

lower BER values for different QFs.

The robustness of the proposed decoder is then investigated under AWGN attack. Fig. 6 shows BER results obtained using the proposed decoder as well as the results provided by the method in [16] for the same set of images under the AWGN with σ_n varying from 15 to 30. It is seen from this figure that the proposed NIG-based decoder is more resistant to any level of noise than the decoder in [16] under the AWGN attack. To compare the performance of the proposed scheme under the AWGN attack, Table III gives BER values obtained using the proposed watermarking scheme and that provided by the schemes in [36], [52] and [53] when the watermarked images are contaminated by various levels of the Gaussian noise. The results in this table confirms that the proposed watermarking scheme provides a considerably better performance in the presence of Gaussian noise as compared to the other methods. To further compare the performance of the proposed decoder under the AWGN attack, Table IV gives BER values obtained using the proposed watermarking scheme and that provided by the schemes in [19] and [30], when the watermarked image contains a 256-bit message. It is seen from this table that the proposed NIG-based scheme is more robust than the other schemes under the AWGN attack.

The performance of the proposed decoder is now compared to that presented in [30] and [39], under rotation attack. Table V gives BER values obtained using the NIG-based decoder when the watermarked images *Barbara*, *Peppers*, *Goldhill* and *Lena* are rotated by $-10°$, $-5°$, $5°$ and $10°$. It is seen from this table that the watermarking scheme using the proposed decoder is more robust against rotation attack than the schemes in [30] and [36].

The performance of the proposed decoder is then compared to that presented in [20] and [54], under median filtering attack. Table VI gives BER values obtained using the NIG-based decoder when median filters of mask size 5×5, 7×7 and 9×9 are applied to the watermarked coefficients containing a 64 bit message for the test images, *Barbara*, *Peppers*, *Goldhill* and *Lena*. It is seen from this table that the watermarking scheme using the proposed decoder is more robust than the schemes in [20] and [54] under median filtering attack using masks of various sizes.

In Table VII, we compare the robustness of the proposed watermarking scheme to that of [30], [36] and [55] when the watermark images *Lena*, *Barbara*, *Baboon* and *Peppers* undergo median filtering with a window size of 3×3, Gaussian filtering with a window size of 3×3 and AWGN with $\sigma_n = 10$ with a message length of 256 bits. It is seen from this table that the proposed NIG-based watermarking scheme is more robust than the other methods by providing lower BER values.

Next, the performance of the proposed decoder is investigated under the scaling attack. Tables VIII gives BER values obtained using the proposed decoder as well as those yielded by the method in [16] under scaling attack. It is seen from this table that the proposed watermarking scheme is more robust against scaling attack with respect to that in [16]. It should be noted that for the scaling attack, we assume that the decoder knows the original size of the image. Therefore, we can resize the attacked watermarked image to its original size and then decode the watermark bits.

We also compare the performance of the proposed NIG-based decoder to that of the method in [16] under the salt & pepper noise. Tables IX gives BER values for the two methods with different noise levels. It can be seen from this table that the watermarking scheme using the proposed decoder is more robust than the scheme in [16] under the salt & pepper noise attack.

Table X gives BER values obtained using the proposed decoder and that provided by the schemes in [30] and [36] when the watermarked images *Lena*, *Goldhill*, *Bridge* and *Peppers* are 5% or 10% cropped, when the message length is 256 bits. It is seen from this table that the proposed NIG-based watermarking scheme is more robust than the other methods against the cropping attack. Table XI gives BER values obtained using the proposed watermarking scheme and that provided by the schemes in [30] and [55] when the watermarked images *Boat*, *Plane*, *Bridge* and *Pirate* are filtered by the median and Gaussian filters with a mask of size

TABLE V
BIT ERROR RATES (%) OBTAINED USING THE PROPOSED WATERMARKING SCHEME AS WELL AS THAT OBTAINED USING THE SCHEMES IN [30] AND [36], UNDER ROTATION ATTACK FOR A FEW OF THE TEST IMAGES, NAMELY, *Lena*, *Goldhill*, *Bridge* AND *Peppers*.

	θ											
	-10			-5			5			10		
	Proposed	[36]	[30]	Proposed	[36]	[30]	Proposed	[36]	[30]	Proposed	[36]	[30]
Lena	4.2	6.16	4.68	2.9	5.39	3.12	2.4	4.38	1.56	3.9	4.78	3.12
Goldhill	3.5	4.16	8.59	1.6	4.50	7.81	2.2	3.04	7.03	3.4	4.06	6.64
Bridge	4.3	9.31	12.89	2.5	7.02	7.81	2.1	7.06	6.24	4.4	9.23	10.93
Peppers	3.1	5.64	5.47	1.4	4.72	5.07	1.3	5.84	2.34	2.9	6.55	3.51

TABLE VI
BIT ERROR RATES (%) OBTAINED USING THE PROPOSED NIG-BASED DECODER AND THE DECODERS IN [20] AND [54] UNDER MEDIAN FILTERING ATTACK USING MASKS OF VARIOUS SIZES (PSNR = 42 *dB*).

	5×5			7×7			9×9		
	Proposed	[20]	[54]	Proposed	[20]	[54]	Proposed	[20]	[54]
Baboon	1.63	1.55	12.50	3.36	4.88	12.50	7.14	8.89	78.13
Peppers	0	0	7.81	0	0	9.36	1.10	3.00	51.56
Goldhill	0	0.77	9.38	0	1.64	9.38	2.87	5.70	69.69
Lena	1.49	-	9.38	4.34	-	12.50	9.08	-	51.56

TABLE VII
BIT ERROR RATES (%) OBTAINED USING THE PROPOSED WATERMARKING SCHEME AS WELL AS THAT OBTAINED USING THE SCHEMES IN [30], [36] AND [55], UNDER VARIOUS KINDS OF ATTACKS FOR A FEW OF THE TEST IMAGES. (MESSAGE LENGTH=256 BITS, PSNR = 42 *dB*)

	Median filter 3×3			Gaussian filter 3×3			AWGN, $\sigma_n = 10$		
	Proposed	[30]	[55]	Proposed	[36]	[55]	Proposed	[30]	[55]
Lena	4.2	6.24	16.56	0	4.73	8.20	0.9	5.01	6.64
Barbara	4.3	19.52	24.49	0	8.71	9.34	1.3	11.47	7.15
Baboon	3.9	17.38	33.63	0	9.80	17.58	0.7	6.13	6.25
Peppers	1.3	8.30	15.63	0	3.55	8.59	1.1	3.62	3.16

TABLE VIII
BIT ERROR RATES (%) OBTAINED USING THE PROPOSED NIG-BASED DECODER AND THE DECODER IN [16] UNDER SCALING ATTACK.

	0.8		1.1		2	
	Proposed	[16]	Proposed	[16]	Proposed	[16]
Barbara	4.11	10.39	3.35	8.28	3.35	8.28
Baboon	6.23	21.37	1.12	3.05	1.12	3.05
Couple	2.32	7.19	0.67	1.88	1.08	1.88
Bridge	2.69	7.85	0.21	0.47	0.21	0.47

TABLE IX
BIT ERROR RATES (%) OBTAINED USING THE PROPOSED DECODER AND THE DECODER IN [16] UNDER SALT & PEPPER NOISE ATTACK.

	1%		3%		5%	
	Proposed	[16]	Proposed	[16]	Proposed	[16]
Barbara	1.53	3.28	2.30	4.18	2.92	4.80
Baboon	0.66	1.91	1.36	2.81	2.14	3.79
Couple	2.84	6.72	5.33	8.55	7.75	10.35
Bridge	1.81	5.43	4.08	7.27	6.12	9.10

TABLE X
BIT ERROR RATES (%) OBTAINED USING THE PROPOSED WATERMARKING SCHEME AS WELL AS THAT OBTAINED USING THE SCHEMES IN [30] AND [36], UNDER CROPPING FOR A FEW OF THE TEST IMAGES, NAMELY, *Lena*, *Goldhill*, *Bridge* AND *Peppers*, (MESSAGE LENGTH=256 BITS).

	5%			10%		
	Proposed	[30]	[36]	Proposed	[30]	[36]
Lena	0.5	0.78	1.83	3.4	5.85	5.92
Goldhill	1.8	6.64	2.84	6.1	13.67	6.53
Bridge	1.6	8.98	4.63	6.7	18.36	13.42
Peppers	0.8	3.51	6.58	5.1	6.25	10.48

is computationally efficient, since its required CPU time averaged over a set of images on an Intel Core $i7$ 2.93 GHz personal computer with 8 GB RAM is 16.70 and 1.06 seconds for the regular and lightweight (with predefined parameters for NIG PDF) versions, respectively.

V. CONCLUSION

In this paper, a new multiplicative watermark decoder in the contourlet domain has been proposed by using the normal inverse Gaussian PDF as a prior for the contourlet coefficients of images. The watermark decoder has been developed using the maximum likelihood criterion in both the clean and noisy

3×3. It is seen from this table that the proposed scheme using the NIG-based decoder is more robust than the other schemes against filtering attack.

In terms of complexity, the proposed NIG-based decoder

TABLE XI
BIT ERROR RATES (%) OBTAINED USING THE PROPOSED SCHEME AS WELL AS THAT OBTAINED USING THE SCHEMES IN [30] AND [55], UNDER MEDIAN AND GAUSSIAN FILTERING WITH A WINDOW SIZE OF 3×3 FOR A FEW OF THE TEST IMAGES, NAMELY, *Boat*, *Plane*, *Bridge* AND *Pirate*.

	Median filter 3×3			Gaussian filter 3×3		
	Proposed	[30]	[55]	Proposed	[30]	[55]
Boat	2.5	7.89	16.42	0	4.69	9.39
Plane	2.7	7.82	11.80	0	3.51	6.80
Bridge	3.9	11.72	13.37	0	5.86	10.16
Pirate	3.1	9.38	11.43	0	5.86	4.69

environments resulting in closed-form analytical expressions for the decoder. The performance of the proposed watermark decoder has been studied in detail by conducting several experiments, and comparing these results with that of the other existing decoders. It has been shown that the proposed decoder provides a more robust decoding performance as its bit error rate is lower than that provided by other existing decoders. The robustness of the proposed watermarking scheme against different attacks such as additive white Gaussian noise, salt & pepper noise, JPEG compression, Gaussian noise, rotation, cropping, Gamma correction and median filtering has been studied and shown to be superior to that of the other existing schemes.

APPENDIX
A. CLOSED-FORM EXPRESSION FOR THE PROPOSED NIG-BASED DECODER IN NOISY ENVIRONMENT

In order to obtain a closed-form expression for the proposed NIG-based decoder in noisy environment, we use numerical integration to simplify (11). To this end, we employ the local Simpsons rule for the reference interval $\left[\frac{-h}{2}, \frac{h}{2}\right]$

$$\int_{\frac{-h}{2}}^{\frac{h}{2}} f(x)dx = \frac{h}{6}\left(f(\frac{-h}{2}) + 4f(0) + f(\frac{h}{2})\right) \quad (A.1)$$

It is seen from (13) that we have two non-zero subintervals in $f_n(n)$ as $[-3\sigma_n, 0]$ and $[0, 3\sigma_n]$. Then (11) can be written as

$$f(\mathbf{z}) = \underbrace{\int_{-3\sigma_n}^{0} f_y(\mathbf{z} - \tau)f_n(\tau)d\tau}_{q_1} + \underbrace{\int_{0}^{3\sigma_n} f_y(\mathbf{z} - \tau)f_n(\tau)d\tau}_{q_2}$$
$$(A.2)$$

Using (A.1) with three interpolation points in each of the subintervals, q_1 and q_2 can be obtained as

$$q_1 = \frac{\sigma_n}{2}(f(\mathbf{z})f_n(0) + 4f(\mathbf{z} - \frac{3\sigma_n}{2})f_n(\frac{3\sigma_n}{2})$$
$$+ f(\mathbf{z} - 3\sigma_n)f_n(3\sigma_n)) \quad (A.3)$$

and

$$q_2 = \frac{\sigma_n}{2}(f(\mathbf{z})f_n(0) + 4f(\mathbf{z} + \frac{3\sigma_n}{2})f_n(\frac{-3\sigma_n}{2})$$
$$+ f(\mathbf{z} + 3\sigma_n)f_n(-3\sigma_n)) \quad (A.4)$$

Inserting the corresponding values of $f_n(n)$, expression for $f(\mathbf{z})$ is obtained and is given as (15).

APPENDIX
B. PARAMETER ESTIMATION OF THE NIG DISTRIBUTION

In order to estimate the parameters α and γ of the NIG distribution, the maximum likelihood (ML) estimation is used as

$$logL(\alpha, \beta, \mu, \delta; X_1, X_2, ..., X_n) =$$
$$\sum_{i=1}^{n} logf_{NIG}(x_i; \alpha, \beta, \mu, \delta) \quad (B.1)$$

where $logL(.)$ is the log-likelihood estimator. We then apply the expectation-maximization (EM) algorithm for ML estimation. The EM-algorithm consists of iterating two steps; the expectation step (E-step) and the maximization step (M-step) [42], [43].

M-Step: In view of the fact that the NIG distribution is a mixed distribution, we can write the joint density of X and Z as $f_{x,z}(x, z) = f_{x|z}(x|z)f_z(z)$. Therefore, the maximum likelihood estimation is rewritten as

$$logL(\alpha, \beta, \mu, \delta; X_1, ..., X_n, Z_1, ..., Z_n) =$$
$$\sum_{i=1}^{n}\left(logf_{x|z}(x_i|z_i; \beta, \mu) + logf_z(z_i; \alpha, \delta)\right) \quad (B.2)$$

For a symmetric and zero-mean distribution, estimating $logL(\alpha, \delta)$ is sufficient. Therefore, we construct the log-likelihood estimation on $f_z(z)$ as

$$logL(\alpha, \delta; Z_1, ..., Z_n) = \sum_{i=1}^{n} logf_z(z_i; \alpha, \delta) \quad (B.3)$$

which can be simplified to

$$logL(\alpha, \delta) = nlog\delta + n\delta\alpha - \frac{\delta^2}{2}\sum_{i=1}^{n}\frac{1}{z_i} - \frac{\alpha^2}{2}\sum_{i=1}^{n}z_i \quad (B.4)$$

Solving (B.4) for δ and α, we have

$$\delta^{(k+1)^2} = \frac{1}{\frac{1}{n}\sum_{i=1}^{n}\frac{1}{z_i} - \frac{n}{\sum_{i=1}^{n}z_i}} \quad (B.5)$$

and

$$\alpha^{(k+1)} = \frac{n\delta^{(k+1)}}{\sum_{i=1}^{n}z_i} \quad (B.6)$$

E-Step: In the E-step, by employing the moments around zero of the generalized inverse Gaussian distribution [42], [43], $E(Z_i|X_i = x_i)$ and $E(Z_i^{-1}|X_i = x_i)$ are given by

$$E(Z_i|X_i = x_i) = \frac{\alpha}{\sqrt{\delta^2 + x_i^2}}\frac{K_0(\alpha\sqrt{\delta^2 + x_i^2})}{K_1(\alpha\sqrt{\delta^2 + x_i^2})} \quad (B.7)$$

and

$$E(Z_i^{-1}|X_i = x_i) = \frac{\sqrt{\delta^2 + x_i^2}}{\alpha}\frac{K_2(\alpha\sqrt{\delta^2 + x_i^2})}{K_1(\alpha\sqrt{\delta^2 + x_i^2})} \quad (B.8)$$

The EM algorithm produces improved parameter estimates in each step. The initial values for EM algorithm are obtained by calculating the sample moments $\bar{m}_i, i = 1, 2, ...$ using the moment generating function $M(t) = E[e^{tx}]$ given by [33], [45],

$$M_{NIG}(x) = \exp\left(\delta(\alpha - \sqrt{\alpha^2 - t^2})\right) \quad (B.9)$$

The second and fourth moments of the NIG distribution are obtained as

$$\bar{m}_2 = \frac{\delta\alpha^2}{\gamma^3}, \quad \bar{m}_4 = \frac{3}{\delta\gamma} \qquad \text{(B.10)}$$

REFERENCES

[1] I. J. Cox, M. L. Miller, and J. A. Bloom, *Digital Watermarking* San Mateo, CA: Morgan Kaufmann, 2001.

[2] G. C. Langelaar, I. Setyawan, and R. L. Lagendijk, "Watermarking digital image and video data: A state-of-the-art overview," *IEEE Transactions on Signal Processing Magazine,* vol. 17, no. 5, pp. 20-46, 2000.

[3] I. J. Cox, J. Kilian, F. T. Leighton, and T. Shamoon, "Secure spread spectrum watermarking for multimedia," *IEEE Transactions on Image Processing,* vol. 6, no. 12, pp. 1673-1687, 1997.

[4] J. Seitz, *Digital Watermarking for Digital Media* Hershey, PA: Information Science, 2005.

[5] C. J. Cheng, W. J. Hwang, H. Y. Zeng and Y. C. Lin, "A fragile watermarking algorithm for hologram authentication," *Journal of display technology,* vol. 10, no. 4, pp. 263-271, 2014.

[6] G. Coatrieux, W. Pan, N. C. Boulahia, F. Cuppens and C. Roux, "Reversible watermarking based on invariant image classification and dynamic histogram shifting," *IEEE Transactions on Information Forensics and Security,* vol. 8, no. 1, pp. 111-120, 2014.

[7] H. Sadreazami, M. O. Ahmad and M. N. S. Swamy, "A study of multiplicative watermark detection in the contourlet domain using alpha-stable distributions," *IEEE Transactions on Image Processing,* vol. 23, no. 10, pp. 4348-4360, 2014.

[8] M. M. Rahman, M. O. Ahmad, and M. N. S. Swamy, "A new statistical detector for DWT-based additive image watermarking using the Gauss-Hermite Expansion," *IEEE Transactions on Image Processing,* vol. 18, no. 8, pp. 1782-1796, 2009.

[9] J. R. Hernndez, M. Amado, and F. P. Gonzlez, "DCT-domain watermarking techniques for still images: Detector performance analysis and a new structure," *IEEE Trans. on Image Process.,* vol. 9, no. 1, pp. 55-68, 2000.

[10] M. Barni, F. Bartolini, A. DeRosa and A. Piva, "Optimum decoding and detection of multiplicative watermarks," *IEEE Transactions on Signal Processing,* vol. 51, no. 4, pp. 1118-1123, 2003.

[11] Q. Cheng and T. S. Huang, "Robust optimum detection of transform domain multiplicative watermarks," *IEEE Transactions on Signal Processing,* vol. 51, no. 4, pp. 906-924, 2003.

[12] Q. Cheng and T. S. Huang, "An additive approach to transform-domain information hiding and optimum detection structure," *IEEE Transactions on Multimedia,* vol. 3, no. 3, pp. 273-284, 2001.

[13] M. Barni, F. Bartolini, and A. Piva, "Improved wavelet-based watermarking through pixel-wise masking," *IEEE Transactions on Image Processing,* vol. 10, no. 5, pp. 783-791, 2001.

[14] A. Briassouli, P. Tsakalides, and A. Stouraitis, "Hidden message in heavy-tails: DCT-domain watermark detection using alpha-stable models," *IEEE Transactions on Multimedia,* vol. 7, no. 4, pp. 700-715, 2005.

[15] T. M. Ng and H. K. Garg, "Maximum- likelihood detection in DWT domain image watermarking using Laplacian modeling," *IEEE Signal Processing Letters,* vol. 12, no. 4, pp. 285-288, 2005.

[16] A. Akhaee, S. M. Sahraeian, and F. Marvasti, "Contourlet-based image watermarking using optimum detector in noisy environment," *IEEE Transactions on Image Processing,* vol. 19, no. 4, pp. 700-715, 2010.

[17] H. Sadreazami, and A. Amini, "A robust spread spectrum based image watermarking in ridgelet domain," *International Journal of Electronics and Communications,* vol. 66, no. 5, pp. 364-371, 2012.

[18] M. Zareian and H. Tohidypour, "Robust quantization index modulation-based approach for image watermarking," *IET Image Processing,* vol. 7, no. 5, pp. 432-441, 2013.

[19] E. Nezhadarya, Z. J. Wang and R. K. Ward, "Robust image watermarking based on multiscale gradient direction quantization," *IEEE Transactions on Information Forensics and Security,* vol. 6, no. 4, pp. 1200-1213, 2011.

[20] A. Akhaee, S. M. Sahraeian, B. Sankur and F. Marvasti, "Robust scaling-based image watermarking using maximum-likelihood decoder with optimum strength factor," *IEEE Transactions on Multimedia,* vol. 11, no. 5, pp. 822-833, 2009.

[21] D. Cheng-Zhi, Z. Huasheng, and W. Sheng-Qian, "Curvelet domain watermark detection using alpha-stable models," *in proc. 5th Inter. Conf. on Information Assurance and Security (IAS),* pp. 313-316, 2009.

[22] M. Jayalakshmi, S. N. Merchant and U. B. Desai, "Digital watermarking in contourlet domain," *in proc. 18th International Conference on Pattern Recognition,* vol. 3, pp. 861-864, 2006.

[23] A. Kumar and V. Kumar, "Blind watermarking in contourlet domain with improved detection," *The International Journal of Multimedia & Its Applications (IJMA),* vol. 3, no. 1, pp. 122-131, 2011.

[24] S. Ghannam, and F. Abou-Chadi, "Contourlet versus wavelet transform: a performance study for a robust image watermarking," *in proc. Inter. Conf. on Image and Vision Computing (IVCNZ),* pp. 545-500, 2009.

[25] S. Ghannam and F. Abou-Chadi, "Enhancing robustness of digital image watermarks using contourlet transform," *in proc. International conference on Image Processing (ICIP),* pp. 3645-3648, 2009.

[26] M. Jayalakshmi, S. N. Merchant, and U. B. Desai, "Blind watermarking in contourlet domain with improved detection," *in proc. International Conference on Intelligent Information Hiding and Multimedia Signal Processing (IIH-MSP),* pp. 449-452, 2006.

[27] H. Song, S. Yu, and C. Wang, "Contourlet-based Image adaptive watermarking," *Signal Process., Image Commun.,* vol. 23, pp. 162-178, 2008.

[28] Y. Bian, S. Liang, "Locally optimal detection of image watermarks in the wavelet domain using Bessel-K form distribution," *IEEE Transactions on Image processing,* vol. 22, no. 6, pp. 2372-2384, 2013.

[29] M. N. Do, *Directional multiresolution image representations,* Ph.D. thesis, School Comput. Commun. Sci., Swiss Fed. Inst. Technol, 2001.

[30] M. Hamghalam, S. Mirzakuchaki and M. A. Akhaee, "Robust image watermarking using dihedral angle based maximum-likelihood detector," *IET Image Processing,* vol. 7, no. 5, pp. 451-463, 2013.

[31] H. Sadreazami, M. O. Ahmad and M. N. S. Swamy, "Contourlet domain image modeling by using the alpha-stable family of distributions," *in proc. Inter. Symp. on Circuits and Systems (ISCAS),* pp. 1288-1291, 2014.

[32] M. Amirmazlaghani, M. Rezghi and H. Amindavar, "A novel robust image watermarking scheme based on Gaussian mixture model," *Expert Systems with Applications,* vol. 42, pp. 1960-1971, 2015.

[33] H. Sadreazami, M. O. Ahmad and M. N. S. Swamy, "Contourlet domain image denoising using the normal inverse Gaussian distribution," *in proc. Canadian Conf. on Elec. and Computer Eng. (CCECE),* pp. 1-4, 2014.

[34] M. I. H. Bhuiyan and R. Rahman, "DCT-domain watermark detection using a normal inverse Gaussian prior," *in proc. 23th Canadian Conference on Electrical and Computer Engineering (CCECE),* pp. 1-4, 2010.

[35] Y. Zhou and J. Wang, "Image denoising based on the symmetric normal inverse Gaussian model and non-subsampled contourlet transform," *IET Image Processing,* vol. 6, no. 8, pp. 1136-1147, 2012.

[36] M. Hamghalam, S. Mirzakuchaki and M. A. Akhaee, "Geometric modeling of the wavelet coefficients for image watermarking using optimum detector," *IET Image Processing,* vol. 8, no. 3, pp. 162-172, 2014.

[37] M. N. Do, and M. Vetterli, "The contourlet transform: an efficient directional multiresolution image representation," *IEEE Transactions on Image Processing,* vol. 14, no. 12, pp. 2091-2106, 2005.

[38] I. Selesnick, R. Baraniuk and N. Kingsbury, "The dual-tree complex wavelet transform," *IEEE Signal Process. Mag.,* vol. 22, no. 6, pp. 123-156, 2005.

[39] E. J. Candes and D. L. Donoho, "Ridgelets: A key to higher-dimensional intermittency," *Philos. Trans. Roy. Soc. London A,* vol. 357, no. 1760, pp. 2495-2509, 1999.

[40] E. J. Candes and D. L. Donoho, "Curvelets- A Surprisingly Effective Non-adaptive Representation for Objects with Edges," *in Curve and Surface Fitting,* C. R. A. Cohen and L. Schumaker, Eds. Nashville, TN: Vanderbilt Univ. Press, 2000.

[41] D. D.-Y. Po and M. N. Do, "Directional multiscale modeling of images using the contourlet transform," *IEEE Transactions on Image Processing,* vol. 15, no. 6, pp. 1610-1620, 2006.

[42] D. Karlis, "An EM type algorithm for maximum likelihood estimation of the normal-inverse Gaussian distribution," *Statistics & Probability Letters,* vol. 57, pp. 43-52, 2002.

[43] T. igrd, A. Hansen, R. Hansen and F. Godtliebsen, "EM-estimation and modeling of heavy-tailed processes with multivariate normal inverse Gaussian distribution," *Signal Process.,* vol. 85, no. 8, pp. 1655-1673, 2005.

[44] A. Eriksson, E. Ghysels and F. Wang, "The normal inverse Gaussian distribution and the pricing of derivatives," *The journal of Derivatives,* vol. 16, no. 3, pp. 23-37, 2009.

[45] A. Hanssen and T. igrd, "The normal inverse Gaussian distribution for heavy-tailed processes," *in proc. IEEE-EURASIP Workshop on Nonlinear Signal and Image processing,* 2001.

[46] H. V. Poor, *An introduction to signal detection and estimation,* 2nd ed. New York: Springer-Verilog, 1994.

[47] S. M. Kay, *Fundamentals of Statistical Signal Processing, Volume II: Detection Theory,* 1st ed. Englewood Cliffs, NJ: Prentice-Hall, 1998.

[48] A. Papoulis, *Probability, Random Variables and. Stochastic Processes,* 3rd edition. New York: McGraw-Hill, 1991.

[49] D. L. Donoho and I. M. Johnstone, "Ideal spatial adaptation by wavelet shrinkage," *Biometrika,* vol. 81, no. 3, pp. 425-455, 1994.

[50] [Online]. Available: http://decsai.ugr.es/cvg/dbimagenes/index.php.

[51] [Online]. Available: http://bows2.ec-lille.fr/

[52] F. Balado, "New geometric analysis of spread-spectrum data hiding with repetition coding, with implications for side-informed schemes," *in proc. Inter. Workshop on Digital Watermarking (IWDW),* pp. 336-350, 2005.

[53] N. Kalantari and S. Ahadi, "A logarithmic quantization index modulation for perceptually better data hiding," *IEEE Transactions on Image Processing,* vol. 19, no. 6, pp. 883-893, 2010.

[54] N. Bi, Q. Sun, D. Huang and J. Huang, "Robust image watermarking based on multiband wavelets and empirical mode decomposition," *IEEE Trans. on Image Process.,* vol. 16, no. 8, pp. 1956-1966, 2007.

[55] M. Akhaee, S. Sahraeian and C. Jin, "Blind image watermarking using a sample projection approach," *IEEE Transactions on Information Forensics and Security,* vol. 6, no. 3, pp. 883-893, 2011.

H. Sadreazami (S'09) received the B.Sc. degree from Khaje Nasir Toosi University (KNTU), Tehran, Iran, in 2007 and the M.Sc. degree from Shahid Beheshti University (SBU), Tehran, Iran, in 2010, both in electrical engineering. He is currently working toward the Ph.D. degree in electrical and computer engineering at Concordia University, Montreal, QC, Canada. He has been a Research Associate in Signal Processing Group at Concordia University from September 2011 where he has worked on statistical modeling with applications on image watermarking and image denoising. His research area includes image and video processing using statistical modeling, medical image denoising and data hiding. He has served as a reviewer for several IEEE journals and major conferences.

M. Omair Ahmad (S'69-M'78-SM'83-F'01) received the B.Eng. degree from Sir George Williams University, Montreal, QC, Canada, and the Ph.D. degree from Concordia University, Montreal, QC, Canada, both in electrical engineering. From 1978 to 1979, he was a Faculty Member with the New York University College, Buffalo, NY, USA. In September 1979, he joined the Faculty of Concordia University as an Assistant Professor of computer science. He joined the Department of Electrical and Computer Engineering, Concordia University, where he was the Chair with the department from June 2002 to May 2005 and is currently a Professor. He holds the Concordia University Research Chair (Tier I) in Multimedia Signal Processing. He has published extensively in the area of signal processing and holds four patents. His current research interests include the areas of multidimensional filter design, speech, image and video processing, non-linear signal processing, communication DSP, artificial neural networks, and VLSI circuits for signal processing. He was a Founding Researcher at Micronet from its inception in 1990 as a Canadian Network of Centers of Excellence until its expiration in 2004. Previously, he was an Examiner of the order of Engineers of Quebec.

Dr. Ahmad was an Associate Editor of the IEEE TRANSACTIONS ON CIRCUITS AND SYSTEMS PART I: FUNDAMENTAL THEORY AND APPLICATIONS from June 1999 to December 2001. He was the Local Arrangements Chairman of the 1984 IEEE International Symposium on Circuits and Systems. In 1988, he was a member of the Admission and Advancement Committee of the IEEE. He has served as the Program Co-Chair for the 1995 IEEE International Conference on Neural Networks and Signal Processing, the 2003 IEEE International Conference on Neural Networks and Signal Processing, and the 2004 IEEE International Midwest Symposium on Circuits and Systems. He was a General Co-Chair for the 2008 IEEE International Conference on Neural Networks and Signal Processing. He is the Chair of the Montreal Chapter IEEE Circuits and Systems Society. He is a recipient of numerous honors and awards, including the Wighton Fellowship from the Sandford Fleming Foundation, an induction to Provosts Circle of Distinction for Career Achievements, and the Award of Excellence in Doctoral Supervision from the Faculty of Engineering and Computer Science of Concordia University.

M. N. S. Swamy (S'59-M'62-SM'74-F'80) received the B.Sc. (Hons.) degree in mathematics from Mysore University, India, in 1954, the Diploma degree in electrical communication engineering from the Indian Institute of Science, Bangalore, in 1957 and the M.Sc. and Ph.D. degrees in electrical engineering from the University of Saskatchewan, Saskatoon, Canada, in 1960 and 1963, respectively. He was conferred in 2009 the title of Honorary Professor at National Chiao Tong University in Taiwan. He is presently a Research Professor and the Director of the Center for Signal Processing and Communications in the Department of Electrical and Computer Engineering at Concordia University, Montreal, QC, Canada, where he served as the Chair of the Department of Elec-trical Engineering from 1970 to 1977, and Dean of Engineering and Computer Science from 1977 to 1993. During that time, he developed the Faculty into a research-oriented one from what was primarily an undergraduate Faculty. Since July 2001, he holds the Concordia Chair (Tier I) in Signal Processing. He has also taught in the Electrical Engineering Department of the Technical University of Nova Scotia, Halifax, and the University of Calgary, Calgary, as well as in the Department of Mathematics at the University of Saskatchewan. He has published extensively in the areas of number theory, circuits, systems and signal processing, and holds five patents. He is the coauthor of six books and three book chapters. He was a founding member of Micronet from its inception in 1990 as a Canadian Network of Centers of Excellence until its expiration in 2004, and also its coordinator for Concordia University.

Dr. Swamy is a Fellow of the Institute of Electrical and Electronics Engineers, Fellow of the Institute of Electrical Engineers (United Kingdom), the Engineering Institute of Canada, the Institution of Engineers (India), and the Institution of Electronic and Telecommunication Engineers (India). In 2008, Concordia University instituted the M.N.S. Swamy Research Chair in Electrical Engineering as a recognition of his research contributions. He was inducted in 2009 to the Provosts Circle of Distinction for career achievements. He has served the IEEE in various capacities such as the President-Elect in 2003, President in 2004, Past-President in 2005, Vice President (Publications) during 20012002, Vice-President in 1976, Editor-in-Chief of the IEEE TRANSACTIONS ON CIRCUITS AND SYSTEMS I from June 1999 to December 2001, Associate Editor of the IEEE TRANSACTIONS ON CIRCUITS AND SYSTEMS during June 1985 to May 1987, Program Chair for the 1973 IEEE CAS Symposium, General Chair for the 1984 IEEE CAS Symposium, Vice-Chair for the 1999 IEEE Circuits and Systems (CAS) Symposium, and a member of the Board of Governors of the CAS Society. He is the recipient of many IEEE-CAS Society awards, including the Education Award in 2000, Golden Jubilee Medal in 2000, and the 1986 Guillemin-Cauer Best Paper Award. He is the Editor-in-Chief of the journal Circuits, Systems and Signal Processing (CSSP) since 1999. Recently CSSP has instituted a best paper award in his name.